Reference: *Biol. Bull.* **216:** 273–292. (June 2009)


# Larval Development With Transitory Epidermis in *Paranemertes peregrina* and Other Hoplonemerteans

SVETLANA A. MASLAKOVA[1,*] AND JÖRN VON DÖHREN[2]

[1]*Oregon Institute of Marine Biology, University of Oregon, Charleston, Oregon 97420; and* [2]*Animal Systematics and Evolution, Freie Universität Berlin, Berlin, Germany*

**Abstract.** We describe development of the hoplonemertean *Paranemertes peregrina* from fertilization to juvenile, using light, confocal, and electron microscopy. We discovered that the uniformly ciliated lecithotrophic larva of this species has a transitory epidermis, which is gradually replaced by the definitive epidermis during the course of planktonic development. The approximately 90 large multiciliated cleavage-arrested cells of the transitory larval epidermis become separated from each other by intercalating cells of the definitive epidermis, then gradually diminish in size and disappear more or less simultaneously. Rudiments of all major adult structures—the gut, proboscis, cerebral ganglia, lateral nerve cords, and cerebral organs—are already present in 4-day-old larvae. Replacement of the epidermis is the only overt metamorphic transformation of larval tissue; larval structures otherwise prefigure the juvenile body, which is complete in about 10 days at 7–10 °C. Our findings on development of digestive system, nervous system, and proboscis differ in several ways from previous descriptions of hoplonemertean development. We report development with transitory epidermis in two other species, review evidence from the literature, and suggest that this developmental type is the rule for hoplonemerteans. The hoplonemertean planuliform larva is fundamentally different both from the pilidium larva of the sister group to the Hoplonemertea, the Pilidiophora, and from the hidden trochophore of palaeonemerteans. We discuss the possible function and homology of the larval epidermis in development of other nemerteans and spiralians in general.

Received 2 November 2008; accepted 4 March 2009.

* To whom correspondence should be addressed, at Oregon Institute of Marine Biology, P.O. Box 5389, Charleston, OR 97420. E-mail: svetlana@uoregon.edu

*Abbreviations:* Ap, apical organ; Cg and CG, cerebral ganglia; CO, cerebral organ; DC, dorsal brain commissure; $EC_D$ , ciliated cell of definitive epidermis; $EC_L$ , ciliated cell of larval epidermis; Ecm, extracellular matrix; Ep, epidermis; Fgt, foregut; GC, gland cell; Gt, gut; lnc, LNC, lateral nerve cord; Mgt, midgut; Ms, body wall muscles; NM, nerve muscles; $Nu_D$, nucleus of definitive epidermis cell; $Nu_L$, nucleus of larval epidermis cell; Oc, ocellus; Pb, proboscis; Pc, posterior cirrus; St, mouth; VC, ventral commissure of cerebral ganglia; Y, yolk.

## Introduction

Nemerteans, commonly known as ribbon worms, are a fascinating but often ignored phylum of marine invertebrates, closely related to coelomate protostome animals with spiral cleavage and trochophore larvae, such as annelids and molluscs. The recent discovery of a modified trochophore larva ("hidden trochophore") in development of a palaeonemertean, *Carinoma tremaphoros* (Maslakova *et al.*, 2004a, b), supports this relationship. The Palaeonemertea appears to be a basal paraphyletic assemblage within the Nemertea. The other two major groups of nemerteans are the stylet-bearing Hoplonemertea and the recently defined clade Pilidiophora, which is characterized by the pilidium larva and includes the Heteronemertea as well as the genus *Hubrechtella*. Hoplonemertea and Pilidiophora appear as monophyletic sister groups on a recent molecular phylogeny of the nemerteans (Thollesson and Norenburg, 2003).

Nemertean development is traditionally categorized into "indirect," meaning development *via* a long-lived planktotrophic pilidium larva, as in most pilidiophoran species for which development is known (*e.g.*, Coe, 1899, 1943; Dawydoff, 1940; Iwata, 1957; Lacalli, 2005), and "direct," usually meaning some kind of uniformly ciliated planuliform larva. This simplistic distinction masks the diversity of development in this phylum. The pilidium has a unique mode of development in which imaginal discs grow and form the adult rudiment within the larval body. It undergoes a catastrophic metamorphosis during which the juvenile

ruptures and devours the larval enclosure (Salensky, 1886, 1912; Cantell, 1966, 1969; Maslakova, pers. obs.). Several pilidiophoran species either have a planktonic nonfeeding larva that does not resemble a typical pilidium (Iwata, 1958; Schwartz and Norenburg, 2005; Megan Schwartz, Seattle University, pers. comm. to SAM) or encapsulated development (Schmidt, 1964). That these all have imaginal discs and some form of metamorphosis (*e.g.,* loss of larval epidermis) suggests that pilidial-type development is ancestral for the Pilidiophora.

When palaeonemerteans and hoplonemerteans are lumped together as "direct developers," what is meant by this is simply that these groups lack the pilidium larva and its drastic metamorphosis, but developmental modes in these groups are neither uniform nor, necessarily, direct in the usual sense. Most studied palaeonemerteans have long-lived, and probably feeding, planktonic larvae, which develop into juveniles gradually and lack a discrete metamorphosis (Smith, 1935; Coe, 1943; Iwata, 1960; Jägersten, 1972; Norenburg and Stricker, 2002). Maslakova *et al.* (2004a, b) discovered that the larva of a palaeonemertean, *Carinoma tremaphoros,* possesses a "hidden prototroch"—a transitory preoral ring of large cleavage-arrested cells derived from the trochoblast cell lineage. The same type of larva is found in *Carinoma mutabilis* (Maslakova, pers. obs.). Thus at least some palaeonemertean larvae appear to be modified trochophores, directly comparable to the trochophore larvae of other spiralians, as defined by the presence of the prototroch derived from the trochoblast cell lineage.

Development of hoplonemerteans, superficially similar to that of palaeonemerteans, is fundamentally different in the fate of larval epidermal cells and blastopore, and in other morphogenetic events. It is also direct in the sense that the transition from the embryo to juvenile does not involve a dramatic change in the body plan or a conspicuous metamorphosis. Some hoplonemerteans have direct development in the sense that they lack a planktonic stage. The young are brooded within the ovaries to an advanced stage (Coe, 1904; Salensky, 1914; Norenburg, 1986; Maslakova and Norenburg, 2008b) or encapsulated embryos develop into fully formed juveniles that crawl out from the egg envelopes (McIntosh, 1873–1874; Iwata, 1960; Maslakova and Malakhov, 1999). However, many species have a nonfeeding planktonic larva, which swims from several days to several weeks before settling (*e.g.,* McIntosh, 1873–1874; Lebedinsky, 1898; Delsman, 1915; Hammarsten, 1918; Coe, 1943; Iwata, 1960; Roe, 1976, 1979, 1993; Stricker and Reed, 1981; Maslakova, pers. obs.). Like the palaeonemertean larvae, hoplonemertean planktonic larvae are opaque and uniformly ciliated and superficially resemble cnidarian planulae, hence the name "planuliform" larva (Norenburg and Stricker, 2002).

Maslakova and Malakhov (1999) reported that the encapsulated embryo of the hoplonemertean species *Tetrastemma candidum* is a "hidden larva," by which they meant that a histologically distinct transitory embryonic epidermis gradually became replaced by the definitive epidermis, indicating metamorphosis of a sort. Transitory epidermis has been also mentioned, even if very briefly, in several other hoplonemerteans, for example *Emplectonema gracile* (Delsman, 1915), *Prostoma graecense* (Reinhardt, 1941), *Argonemertes australiensis* (Hickman, 1963), *Prosadenoporus floridensis* (Maslakova and Norenburg, 2008b), and *Quasitetrastemma stimpsoni* (Magarlamov and Chernyshev, 2009). Its presence, although not specifically mentioned, can also be inferred from the illustrations of the development of *Tetrastemma vermiculus* and *Drepanophorus spectabilis* (Lebedinsky, 1898). Maslakova and Malakhov (1999) hypothesized that this process might be homologous to the loss of larval epidermis in pilidial metamorphosis, which would suggest that hoplonemerteans ancestrally had a pilidial-type development and the extant forms retained a shortened version of metamorphosis, similar to the modified development of such pilidiophoran species as *Micrura akkeshiensis* (Iwata, 1958) and *Poseidon* (=*Lineus*) *viridis* and *P. ruber* (Schmidt, 1964). However, lack of detailed descriptions of morphology, ultrastructure, and fate of the cells of the transitory and definitive epidermis in hoplonemertean development does not allow a solid conclusion about the nature of this process and its possible homology in development of other nemerteans or spiralians in general.

Here we describe in detail the larval development of a hoplonemertean, *Paranemertes peregrina* Coe, 1901, and illustrate the gradual replacement of the transitory larval epidermis in this species by the definitive epidermis. Additionally, we report the presence of a homologous, although not identical, structure in the encapsulated development of another hoplonemertean, *Antarctonemertes phyllospadicola* (Stricker, 1985), and the planktonic development of a third hoplonemertean species, *Oerstedia dorsalis* (Abildgaard, 1806). We discuss the possible function of the transitory epidermis and the implications of our findings for understanding the evolution of development in nemerteans. We also describe the development of internal organs in *Paranemertes peregrina*; our findings differ from the previous accounts of formation of the digestive system, nervous system, and the proboscis during hoplonemertean development.

## Materials and Methods

### *Collecting adults, obtaining gametes, and rearing larvae*

*Paranemertes peregrina* is a common intertidal species in the vicinity of San Juan Island, Washington, and can be easily identified by its characteristic external appearance (Fig. 1A) and spirally sculptured stylets (Roe *et al.*, 2007). Reproductive adults of *P. peregrina* were collected from February through April 2007 from three locations on San

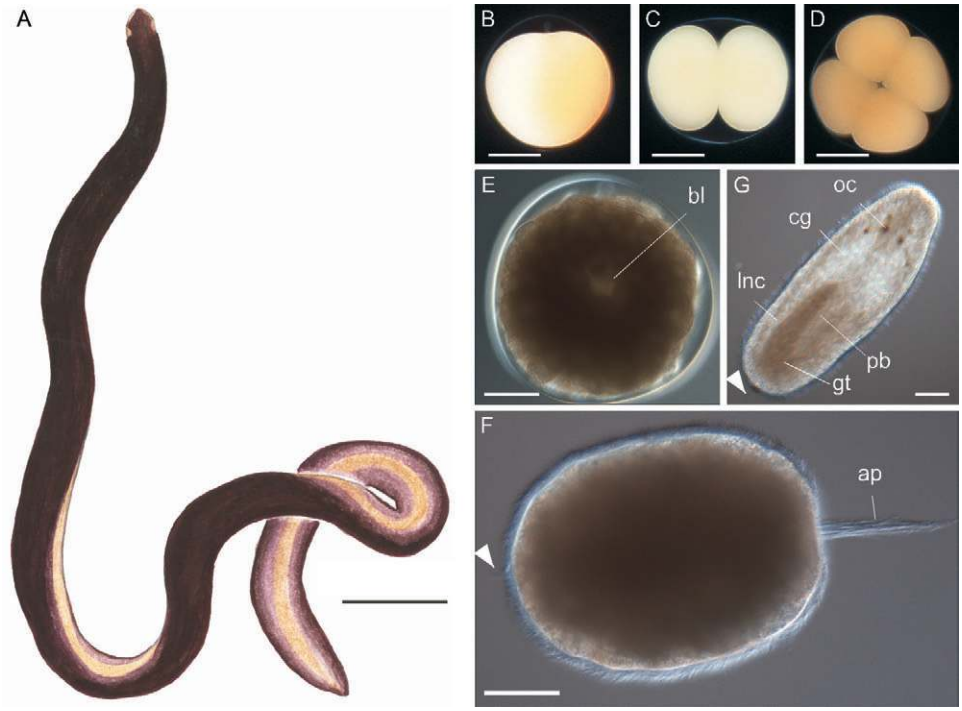


**Figure 1.** Life cycle of a hoplonemertean, *Paranemertes peregrina*. (A) External appearance of the adult worm. Scale bar 3 mm. (B–D) Free-spawned large yolky eggs are surrounded by a tight chorion and undergo equal spiral cleavage. Scale bars 100 μm. (B) Polar body formation. (C) Two-cell stage. (D) Four-cell stage. (E) Narrow opening of the blastopore (bl) is apparent at 22 h after fertilization (at 9–10 °C). Scale bar 65 μm. (F) Four-day-old planuliform planktonic larva is opaque, uniformly ciliated, and possesses a prominent apical tuft (ap) and a short posterior cirrus (arrowhead). Scale bar 75 μm. (G) Ten-day-old juvenile possesses well-developed adult structures, visible through the body wall: large cerebral ganglia (cg), lateral nerve cords (lnc), gut (gt), proboscis (pb), and four to six ocelli (oc). Scale bar 50 μm.

Juan Island: False Bay, Snug Harbor, and Cattle Point. In False Bay and Snug Harbor, individuals of *P. peregrina* can be found crawling on the surface of the sand and underneath blades of *Ulva* at low tide, especially on overcast days; they leave distinct mucous tracks on the surface and can be spotted at the end of such a track. At Cattle Point, *P. peregrina* was found in muddy gravel under rocks and in rock fissures. Once in the laboratory, adults were kept in a small aquarium with a 2–3-cm layer of sand, set in the sea table with running seawater. Water in the aquarium was changed daily.

Oocytes were obtained from two instances of spawning. On one occasion a female spawned in the field after being collected and placed in a 50-ml tube with seawater. In the laboratory, oocytes were rinsed with filtered seawater and fertilized with a diluted solution of sperm obtained by dissecting a male. On another occasion eggs loosely connected by jelly were found in the aquarium with adults, directly on the surface of the sand, the morning after nemerteans were collected. Males and females were kept together, and the eggs were found already fertilized and in the process of producing polar bodies. Oocytes obtained by dissecting ripe females could not be successfully fertilized. On several occasions, eggs were found in a container with fragmenting females, but the fertilization success with these eggs was very low. All the observations in this study were based on larvae from the two spawning events described above. Fertilized eggs were kept in custard dishes with filtered seawater (0.45 μm) in a sea table with running seawater. Water was changed two or three times a week. Sea table temperature ranged from 7.5 °C to 10 °C during the study period.

*Antarctonemertes phyllospadicola* (Stricker, 1985) is a small (up to 12 mm long) yellowish-brown to orange hoplonemertean with four eyes and a prominent snout. It is commonly found on blades and inside female inflorescences of the surfgrass *Phyllospadix scouleri* Hooker in the low horizon of the rocky intertidal on the west coast of San Juan Island, Washington. Egg cocoons and reproductive adults of *A. phyllospadicola* were collected by SAM in June 2004, July 2007, and July 2008 from the inflorescences of *P. scouleri* in the low intertidal zone at Cattle Point, San Juan Island. Development of this species takes several weeks and is entirely encapsulated. Embryos that hatched from the egg chorions (hatchlings) were removed from the cocoons with sharp forceps before fixation and staining.

Reproductive adults of *Oerstedia dorsalis* were collected by SAM intertidally in the vicinity of the Marine Biological Laboratory in Woods Hole, Massachusetts, in June 2000 and July 2002 from the root masses and blades of sea grass. Sea grass was submerged in a bucket of seawater for 30 min to a few hours at room temperature. Nemerteans crawling up to the water surface were picked out and identified by SAM. Several males and females of *O. dorsalis* were placed together in 200-ml custard dishes with daily exchanges of filtered seawater and left at room temperature. Nemerteans usually laid small egg masses (containing a few dozen eggs each) loosely connected by jelly, the morning after or within the first few days of being collected, often shortly after a water change or a change in light conditions. Developing embryos and larvae were kept in custard dishes with daily exchanges of filtered seawater.

### *Phallacidin labeling and confocal microscopy*

Prior to fixation, larvae were relaxed in a 1:1 mixture of 0.33 mol $l^{-1}$ $MgCl_2$ and filtered seawater for 10–15 min at room temperature. Larvae were fixed for 20–30 min at room temperature in 4% paraformaldehyde freshly prepared from 16% ultrapure paraformaldehyde (Electron Microscopy Sciences) and filtered seawater. After fixation, larvae were either rinsed in three 10-min changes of phosphate buffered saline (PBS) pH 7.4 (Fisher Scientific) and stored in PBS at 4 °C or immediately permeabilized and stained with phallacidin.

For confocal microscopy, larvae were permeabilized in three 10-min changes of PBS with 0.1% Triton X-100 (Fisher Scientific), hereafter referred to as PBT, then stained with Bodipy FL phallacidin (1U/100 $\mu$l of PBT) for 40 min at room temperature. In a few cases we added Sytox Green diluted 1:5000 or 1:10000 for the last 5 min of incubation with phallacidin. After staining, larvae were rinsed in three 10-min changes of PBS and mounted on poly-L-lysine coated coverslips supported by 200-$\mu$m-thick adhesive foil tape over glass slides. To visualize outlines of epidermal cells, larvae were mounted in Vectashield (Vector Laboratories) and the preparations sealed with nail polish. To examine internal morphology, larvae were mounted on poly-L-lysine coated coverslips, quickly dehydrated in isopropanol (1 min 70%, 1 min 85%, 1 min 95%, 1 min 100%, 1 min 100%), cleared in three 10-min changes of Murray Clear, mounted in Murray Clear on glass slides with 200-$\mu$m-thick tape supports, and sealed with nail polish.

Hatchlings of *Antarctonemertes phyllospadicola*, removed from the egg cocoons, were fixed in 4% paraformaldehyde in seawater overnight at 4 °C, permeabilized in PBT (as above), and stained with Bodipy FL phallacidin for 1.5 h at room temperature. To determine the pattern of ciliation, some hatchlings were double-labeled with phallacidin and anti-tubulin antibody. For this, fixed and permeabilized hatchlings were blocked in 5% normal goat serum for 2 h at room temperature, rinsed in three 10-min changes of PBT, and stained in 1:1000 rat anti-alpha-tubulin antibody (AbD Serotec # MCA 77G) in PBT overnight at 4 °C. After incubation with the primary antibody, hatchlings were rinsed in three 10-min changes of PBT and then incubated with 1:1000 goat-anti-rat Alexa Fluor 568 secondary antibody (Molecular Probes/Invitrogen #A11077) and 1U/200 $\mu$l phallacidin diluted in PBT. Stained specimens were rinsed in three 10-min changes of 1X PBS, mounted in Vectashield on poly-L-lysine coated coverslips suspended over glass slides, and sealed with nail polish.

Stained samples were examined with a BioRad Radiance 2000 laser scanning confocal system mounted on a Nikon Eclipse E800 microscope using a 40× 1.3 NA oil immersion lens. Stacks of 1-$\mu$m optical sections were imported into ImageJ ver. 1.42i (Wayne Rasband, NIH) for three-dimensional reconstructions and further image processing. Surface cell counts for phallacidin-labeled Murray-cleared *Paranemertes peregrina* larvae were performed in Voxx (Indiana University) and ImageJ by creating epidermal roll-out maps (Appendix Fig. 1).

### *Scanning electron microscopy*

For scanning electron microscopy, hatchlings of *Antarctonemertes phyllospadicola* were dissected from the egg cocoons and fixed for 1 h i n2.5% glutaraldehyde in 0.2 mol $l^{-1}$ sodium cacodylate buffer (pH 7.4) by doubling the volume of seawater containing embryos with 5% glutaraldehyde in sodium cacodylate buffer. Embryos were rinsed in three 10-min changes of fixation buffer; postfixed for 1 h in 2% $OsO_4$ freshly diluted in fixation buffer from 4% stock (from a sealed glass ampoule, Electron Microscopy Sciences); rinsed in two quick changes, three 10-min changes, and one 30-min change of deionized water; dehydrated through an ethanol series (30%, 50%, 70%); and stored in 70% ethanol. Embryos were further dehydrated in 80% ethanol, two changes of 95% ethanol, and three changes of 100% ethanol; critical-point dried using an Emscope CPD 750; mounted on stubs; gold-sputtered in an Emscope SC500; and imaged on a Tescan Vega digital scanning electron microscope.

### *Transmission electron microscopy*

Larvae were fixed in 1.25% glutaraldehyde in 0.05 mol $l^{-1}$ phosphate buffer with 0.3 mol $l^{-1}$ sodium chloride (pH 7.2, 4 °C) for 60 min, rinsed in phosphate buffer, and postfixed in 1% $OsO_4$ in phosphate buffer (4 °C) for 60 min. Samples were dehydrated in an acetone series, embedded in Embed-812 (Electron Microscopy Sciences) according to the standard protocol (von Döhren and Bartolomaeus, 2006), and sectioned into 60-nm silver interference colored sections with a diamond knife on a Reichert Ultracut S

microtome. Sections were mounted on Formvar-covered single-slot copper grids, automatically stained with uranyl acetate and lead citrate (Phoenix Autostainer (Nanofilm), and examined in a Philips CM120 BioTWIN transmission electron microscope. Images were digitally recorded on Ditabis image plates.

*DNA extraction, PCR amplification, and sequencing*

With the purpose of clarifying the taxonomic position of *Antarctonemertes phyllospadicola* (Stricker, 1985), we extracted the DNA of three worms from Cattle Point (San Juan Island, WA) using a DNEasy Blood and Tissue Kit (Qiagen), and PCR-amplified partial sequence of the "barcoding" mitochondrial gene cytochrome oxidase subunit I directly from genomic DNA using universal primers: LCO1419 [GGTCAACAAATCATAAAGATATTGG] and HCO2198 [TAAACTTCAGGGTGACCAAAAAATCA] (Folmer *et al*., 1994). PCR was carried out in 20-$\mu$l reactions with 1U/Rx of Go Taq polymerase in supplied buffer (Promega), 200 $\mu$mol $l^{-1}$ dNTPs, 500 nmol $l^{-1}$ of each primer, and the following cycling parameters: 95 °C 2 min, followed by 35 cycles of 95 °C 40 s, 52 °C 40 s, 72 °C 1 min, and final extension at 72 °C for 2 min. PCR products were purified using a Wizard SV Gel and PCR Clean-up System (Promega), gel-quantified using Low Molecular Weight DNA Ladder (New England Biolabs), labeled using BigDye Terminator ver. 3.1 Cycle Sequencing kit chemistry (Applied Biosystems), and sequenced in one direction on a 3130XL genetic analyzer (Applied Biosystems). Sequences were checked for quality and trimmed to 627 bp using Codon Code Aligner ver. 3.01 (Codon Code Corporation). The sequence from one specimen differed from the other two in having a synonymous transition (C-T) at position 570 (both variants with Phred quality scores above 40). Sequences of both haplotypes have been submitted to GenBank (accession numbers FJ594418, FJ594419).

## Results

*Larval development of* Paranemertes peregrina

Spawned oocytes of *Paranemertes peregrina* were round, opaque, and slightly pinkish. Oocytes observed through the body wall of numerous reproductive females varied from yellowish and pale pinkish to darker shades of rose or even brownish. Oocytes from one of the spawning events measured 240 $\mu$m in diameter and were surrounded by an egg chorion 275 $\mu$m in diameter and a jelly coat 800 $\mu$m in diameter on average ($n = 5$). Fertilized eggs underwent equal spiral cleavage (Fig. 1B–D). Two polar bodies were observed by 2 h 30 min after fertilization (9–10 °C). First cleavage was observed at 3 h 10 min (10 °C) and 3 h 50 min (9 °C) after fertilization, and 2nd cleavage at 4 h 30 min (10 °C) and 5 h 10 min (9 °C) after fertilization. Embryos were at the 8-cell stage by 7 h after fertilization (9 °C). A deep and narrow blastopore opening was observed in round non-ciliated 22-h-old embryos at 10 °C (Fig. 1E).

Bullet-shaped uniformly ciliated larvae with a thin apical tuft hatched and actively swam by 50 h at 10 °C. At 4 days, larvae became somewhat more elongated, actively swam, and had a prominent apical tuft originating from the apical organ (Fig. 1F). Five days after fertilization, we were able to discern rudiments of most adult organs on confocal sections of phallacidin-labeled larvae: proboscis and rhynchocoel, cerebral ganglia and lateral nerve cords, cerebral organs, mouth, foregut and midgut. By 8 days of development, larvae developed functional musculature and became contractile. When relaxed in $MgCl_2$, larvae measured about 450 $\mu$m long and 200 $\mu$m wide.

Ten-day-old specimens of *Paranemertes peregrina* looked like young nemertean worms, each with an apical tuft and a short posterior ciliary cirrus. They possessed four to six subepidermal reddish-brown ocelli and well-developed cerebral ganglia, lateral nerve cords, and proboscis, which were clearly visible through the body wall (Fig. 1G). At this point, juveniles were positively phototactic; they mostly crawled on the bottom of the culture dish, but actively swam when disturbed. Two-week-old juveniles measured about 550 $\mu$m long and 160 $\mu$m wide, and by 3 weeks were about 600 $\mu$m long and 150 $\mu$m wide. Three-week-old juveniles had 4–6 ocelli and developed proboscis armature, consisting of a central stylet on a basis and two pouches with accessory stylets. The apical tuft was reduced but still discernible. Juveniles were capable of swimming if stirred up from the bottom of culture dishes.

*Transitory larval epidermis in* Paranemertes peregrina

We used fluorescent phallacidin and confocal microscopy to visualize outlines of the epidermal cells, revealing that almost the entire surface of the newly hatched 2-day-old larvae is covered by a relatively small number (86–92, average 88, $n = 5$) of large (up to 50 $\mu$m across or more), irregularly shaped cells. The slight difference in the total number of large cells counted in different larvae could be a result of developmental asynchrony or of ambiguity about which cells to count as "large." In these larvae a few small cells (2–5 $\mu$m across) appear in between some of the large cells (Figs. 2A–C, L; Appendix Fig. 1). The apical organ located at the anterior end appears as a small invagination, brightly labeled with phallacidin and surrounded by four large epidermal cells (Fig. 2L) aligned with the primary symmetry planes of the larva (the plane of bilateral symmetry and the perpendicular midfrontal plane). The other epidermal landmarks include the midventral mouth, surrounded by a rosette of 9–10 large cells (Fig. 2A), and the paired cerebral organs (Fig. 2C, L). Two lateral cerebral organ pores are located anteriorly near the apical organ (Fig.

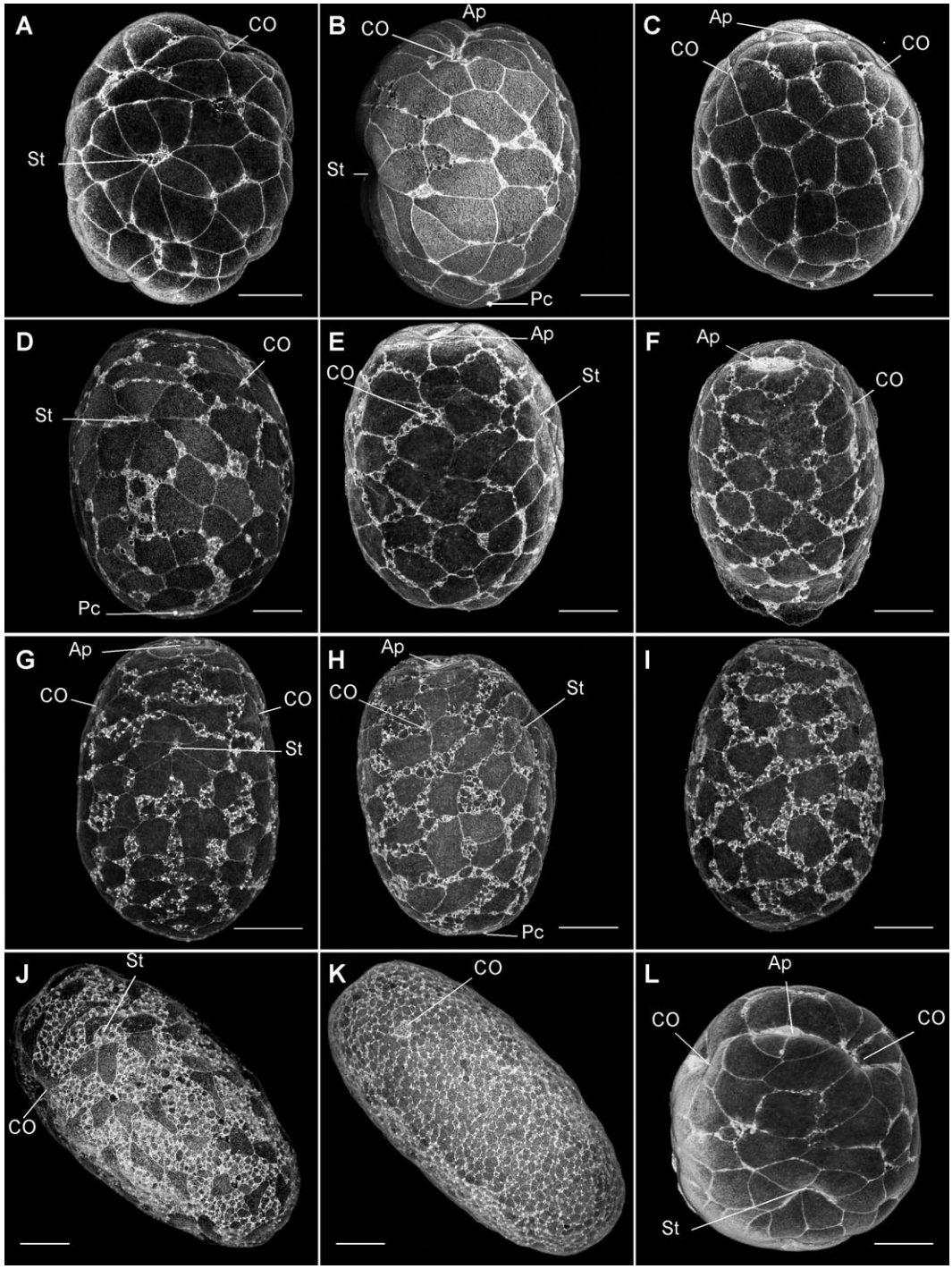


**Figure 2.** Confocal z-projections of phallacidin-labeled planktonic planuliform larvae of *Paranemertes peregrina*, showing outlines of epidermal cells and illustrating gradual replacement of the transitory larval epidermis (large cells) by the definitive epidermis (small cells). Prominent epidermal landmarks include the apical organ (Ap), paired cerebral organs (CO), ventral mouth (St), and posterior cirrus (Pc). Left panels, ventral view; middle panels, lateral view; right panels, dorsal view, except for L. Apical pole is up on all panels (upper left in J and K). (A–C) Two-day-old larvae recently hatched from egg envelopes; the majority of the larval surface is covered by the few (about 90) large cells of larval epidermis. (D–F) Four-day-old larvae, in which small columnar cells of the definitive epidermis begin to intercalate between the cells of the larval epidermis. (G–I) Five-day-old larvae with increased number of definitive epidermal cells and the same number (about 90) of larval epidermal cell in earlier stages. (J) Eight-day-old larva in which irregularly shaped cells of larval

2A–C, L). The exact number, shape, and arrangement of cells around the mouth varied between larvae, but the pattern was characteristic enough to unambiguously identify the position of the mouth in every specimen at all developmental stages we investigated (Fig. 2A–B, D, G, J, and L).

Four-day-old larvae (Fig. 1F) were similar to newly hatched larvae but possessed a more prominent apical tuft. Confocal Z-projections of phallacidin-labeled larvae show numerous very small cells intercalating between the large cells of the larval epidermis (Figs 2D–F), while the number of the large cells remains remarkably unchanged (85, $n = 1$), suggesting that these cells are cleavage-arrested. The mouth narrowed and only about 5–6 surface cells appeared to maintain contact with it (Fig. 2D). Subsequent development resulted in a progressive increase in the number of small cells and a gradual decrease in the size and total surface area covered by the large cells, as shown for 5-day-old (Fig. 2G–I, Appendix Fig. 1) and 8-day-old larvae (Fig. 2J), while the number of large cells remained the same in 5-day-old larvae (85–86, $n = 3$) and slightly decreased in 8-day-old larvae (82, $n = 1$). Finally, in 10-day-old juveniles (which were mostly crawling on the bottom of the culture dish although they could still swim), the entire surface was composed of small cells of definitive epidermis, while the large cells of the larval epidermis were no longer present (Fig. 2K).

Ultrastructural analysis of the larval epidermis in 4-day-old larvae showed that the cells of transitory larval epidermis are filled with yolk granules and have a large euchromatic nucleus (7–10 $\mu$m in diameter) with a prominent nucleolus or two (1–2 $\mu$m in diameter), suggesting lack of mitotic activity (Fig. 3A). Cells of the transitory epidermis are connected by adhaerens junctions to each other and the intercalating smaller cells of the definitive epidermis (Fig. 3A inset, 3B) and possess numerous microvilli and cilia (Fig. 3A, B), the latter apparent even with light microscopy (Fig. 1F). At this and earlier stages, no continuous basal lamina could be detected underneath the epidermis, only some isolated patches of the extracellular matrix at the base of some of the definitive epidermis cells (Fig. 3D). The definitive epidermis cells intercalating between the transitory epidermis cells are much smaller (2–5-$\mu$m apical width) and possess smaller nuclei (2–3 $\mu$m in diameter) with a large amount of heterochromatin (Fig. 3C). Cytoplasm of the cells of definitive epidermis contains numerous mitochondria and centrioles, the latter indicating ciliogenesis (Fig. 3B–C). Definitive epidermis cells also contain yolk granules and are equipped with apical cilia and microvilli (Fig. 3B, E).

In 8-day-old larvae, the large transitory epidermal cells, which at this stage occupy only a fraction of the surface (Fig. 2J), display characteristic signs of degradation, such as clusters of stacked membranes, irregularly shaped vacuoles, and pycnotic nuclei (Fig. 3E). Definitive epidermis includes ciliated cells as well as mucous gland cells (Fig. 3E) and serous gland cells (not shown). Ciliated cells of the definitive epidermis appear to have more microvilli and cilia per unit of surface area and smaller yolk vesicles compared to the transitory epidermis cells. At this stage, epidermis rests on a continuous basal lamina (Fig. 3E). The basal lamina develops only at the stage when the cells of the transitory epidermis start disappearing, and we did not observe those cells in direct contact with the basal lamina. Nevertheless, we refer to them as epidermal cells because they are ciliated, connected with adhaerens junctions, and serve as epidermis in early larval development.

### *Development of the internal organs in* Paranemertes peregrina

*Digestive system.* The blastopore was visible as a narrow opening in 22-h old embryos (Fig. 1E). Within the next day the blastopore closed, sealing off the primordial gut while the mouth appeared as a separate invagination on the ventral side (Fig. 2A–B, L). In 4-day-old larvae, this invagination leads into a pouch-like foregut (Fig. 4A–B). The midgut has a separate lumen, disconnected from the foregut (Figs. 4A–D; 5A–B). The foregut and the midgut fuse by 5 days of development (Figs. 5C–D; 6C, E) and are further integrated in the 8-day-old larvae (Figs. 5E–F; 7A, C, and F). We did not observe the anus in 2-week old larvae, only a small epidermal invagination at the posterior end (data not shown).

*Proboscis and rhynchocoel.* The proboscis rudiment was first observed as an internal spherical mass of cells with a small lumen close to the anterior end in 2-day-old larvae (Fig. 8A). In 4- and 5-day-old larvae, it appeared as a distinct tubular structure, encircled by the developing brain ring (Figs. 4A–D; 5A–D; 6D–F). We have not observed an actual epidermal invagination associated with the proboscis rudiment, although it is possible that it is present in earlier stages (before hatching). We observed two layers of cells surrounding the proboscis rudiment, which likely represent the rudiment of the rhynchocoel (Figs. 4A; 6D, F). The

epidermis are still visible but reduced in size and mostly separated from each other by numerous intercalating small cells of the definitive epidermis. (K) Ten-day-old juvenile, in which cells of larval epidermis are no longer present and the entire epidermis consists of small cells. (L) A two-day-old larva viewed from the anteroventral side looks grumpy. Scale bars 50 $\mu$m.

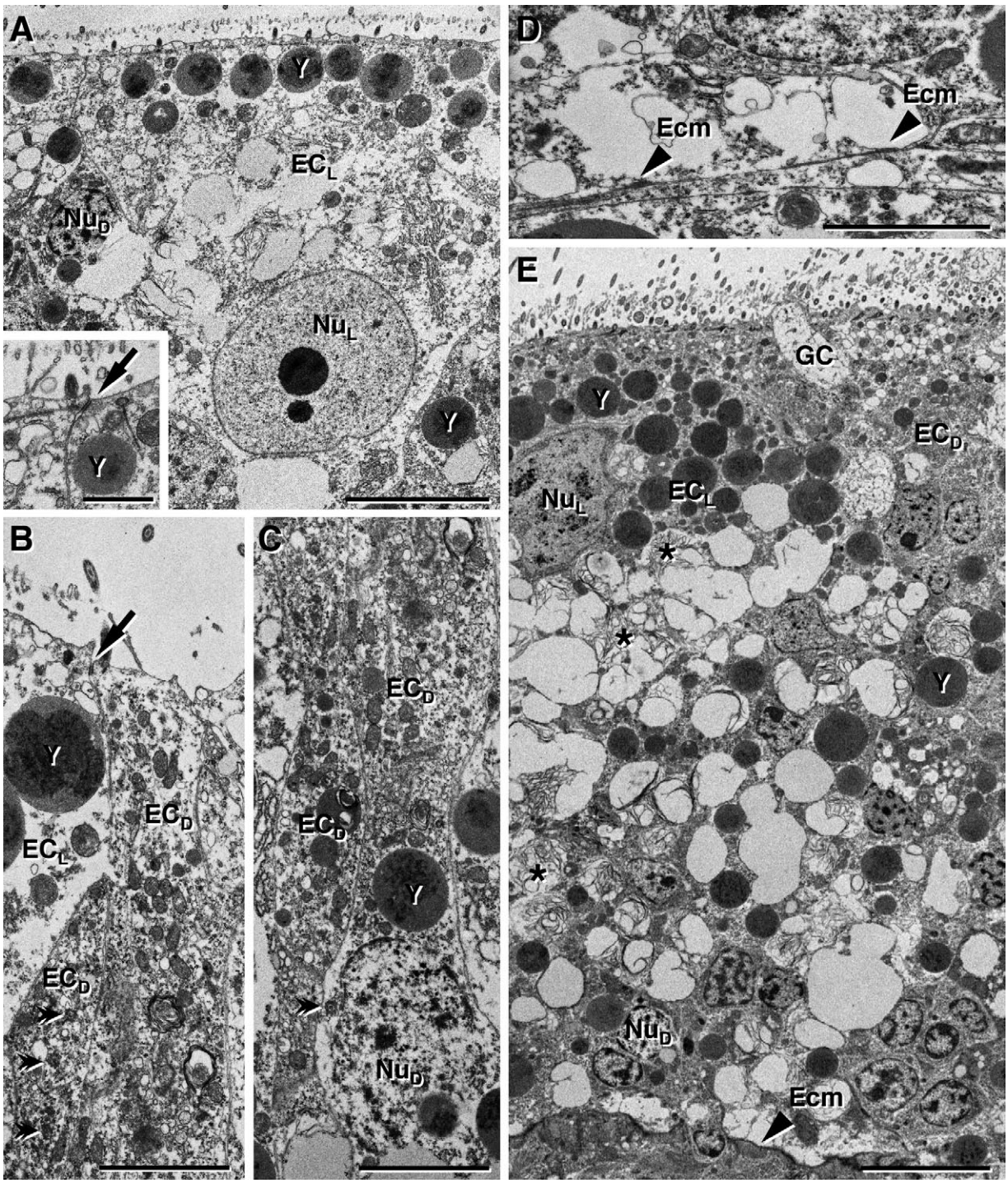


**Figure 3.** Transmission electron microscopy of epidermis in 4-day-old (A–D) and 8-day-old (E) larvae of *Paranemertes peregrina*. (A) A large cell of transitory larval epidermis ($EC_L$) contains numerous yolk granules (Y) and a large nucleus ($Nu_L$) with two prominent nucleoli. Cells of the transitory epidermis are connected by adhaerens junctions (inset, arrow). (B–C) Two of the prospective ciliated cells of the definitive epidermis ($EC_D$) are intercalating between the cells of the transitory epidermis. They are connected to the surrounding cells by the apical adhaerens junctions (arrow) and contain numerous mitochondria, centrioles (double arrowheads)—which presumably will act as basal bodies of future cilia—and relatively small heterochromatin-rich nuclei ($Nu_D$). (D) Basal lamina is only starting to develop at this stage and is represented by discontinuous patches of extracellular matrix (arrowheads, Ecm). (E) Definitive epidermis of the 8-day-old larva rests on a well-developed

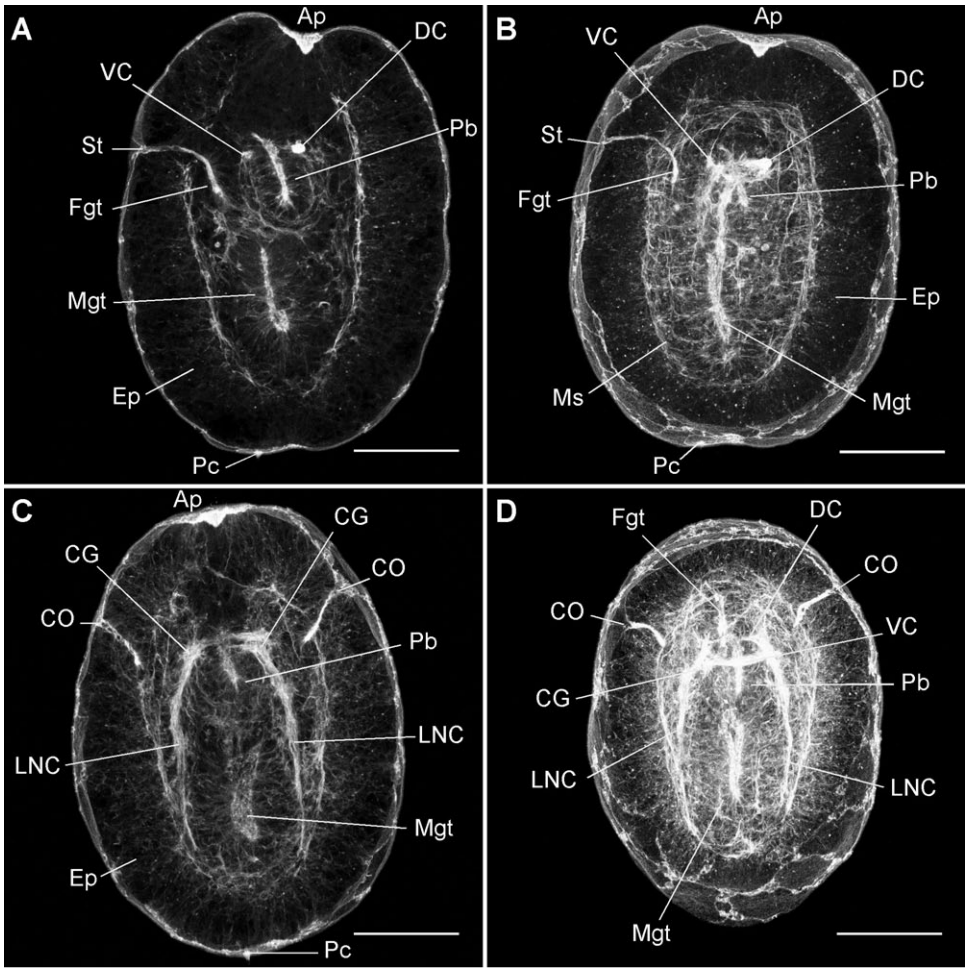


**Figure 4.** Internal anatomy of the phallacidin-labeled 4-day-old larvae of *Paranemertes peregrina* is revealed in confocal z-projections of sub-stacks of 1-$\mu$m optical sections, chosen to illustrate major morphological structures. The apical organ (Ap) marks the anterior end, and the posterior cirrus (Pc) marks the posterior end. The groundplan of the nervous system is established by 4 days. It includes the cerebral ganglia (CG), connected by the dorsal (DC) and ventral commissures (VC), and the two lateral nerve cords (LNC). The proboscis (Pb) appears as the tubular structure dorsal to the foregut (Fgt) and anterior to the midgut (Mgt); it penetrates the brain ring. The developing body-wall muscles (Ms) mark the thickness of the epidermis (Ep), which is about half of the larval diameter. Each panel is a different larva. Apical pole is up. (A) Sagittal sections, 10-$\mu$m sub-stack. (B) Sagittal sections, 50-$\mu$m sub-stack. The mouth (St) leads into the foregut (Fgt), which is not yet connected to the midgut (Mgt). (C and D) Frontal sections, 60-$\mu$m sub-stacks. The two deep lateral invaginations at the anterior end are the cerebral organs (CO)—prominent anatomical landmarks in larvae of *P. peregrina*. Scale bars 50 $\mu$m.

proboscis continues to elongate, reaching 75–80 $\mu$m in length in the 8-day-old larvae, and develops a delicate layer of muscle fibers (Figs. 5E–F; 7D, F). The proboscis opens into the rhynchodaeum, which connects to the foregut later in development, so that the juvenile mouth and the proboscis pore end up sharing a common opening—the rhynchostomopore. Proboscis stylets were observed in 3-week-old juveniles.

*Cerebral organs.* Rudiments of the cerebral organs were first observed in phallacidin-labeled 2-day-old larvae of *Paranemertes peregrina*. They appear as a pair of shal-

basal lamina (arrowhead, Ecm) and contains multiciliated cells ($EC_D$) and gland cells (GC). A large cell of the transitory epidermis shows signs of degradation—pycnotic nucleus and numerous vacuoles with stacks of membranes (asterisks). Scale bars: A and E, 5 $\mu$m (inset, 1$\mu$m); B–D, 2 $\mu$m.

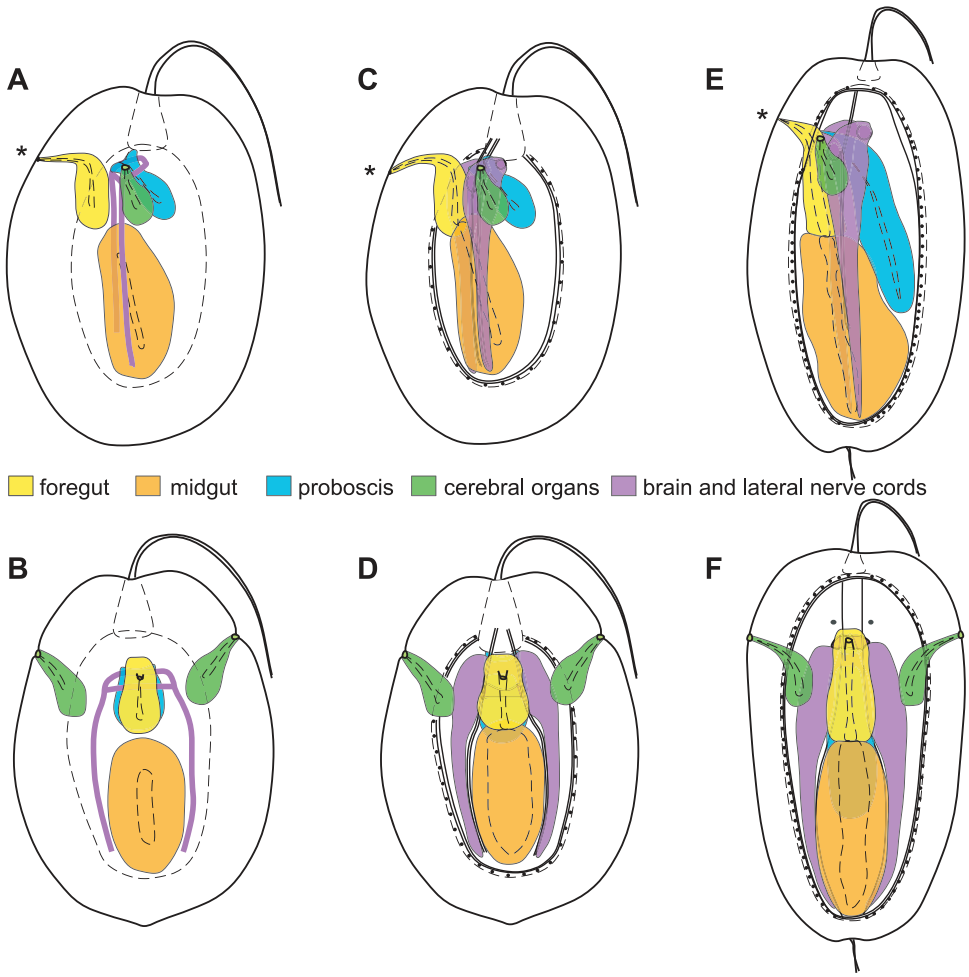


**Figure 5.** Diagrams of 4-day-old (A and B), 5-day-old (C and D), and 8-day-old (E and F) larvae of *Paranemertes peregrina* summarizing development of major internal organs. The ectodermally derived foregut and the endodermally derived midgut fuse by 5 days of development. The basic plan of the nervous system is established by 4 days of development. The proboscis is a simple tubular structure that penetrates the brain ring and gradually elongates. The cerebral organs are the two lateral sacks located close to the brain. Apical pole up. A, C, and E—lateral view. B, D, and F—ventral view. Mouth marked with an asterisk.

low lateral epidermal invaginations at the anterior end (Figs. 2A–C, L; 8A–B). Within the next 2 days of development, cerebral organ invaginations deepen and their distal portions penetrate the newly formed body-wall muscles, arriving close to the developing cerebral ganglia (Figs. 4C–D; 5A–D; 6A–C), where they are found in the adult worms. The cerebral organ canals open to the outside *via* tiny lateral pores (Fig. 2D–H) in 4- and 5-day-old larvae. The cerebral organs served as prominent internal landmarks in 8-day-old larvae (Figs. 5E–F; 7A, C). The cerebral organ canal pores are easily identifiable on the confocal projections of the phallacidin-labeled 10-day-old juveniles due to the smaller size of cells lining the cerebral organ canals, as compared to the cells of the definitive epidermis (Fig. 2K). We also observed the cerebral organs in confocal sections of 2-week-old juveniles (not shown).

*Nervous system.* Development of the nervous system was not specifically addressed in this study, but conveniently, phallacidin highlights the fibrous core (axons) of major nerves, which allowed us to provide an outline of the development of the cerebral ganglia, brain commissures, and lateral nerve cords. In 2-day-old larvae there were no distinguishable nervous elements highlighted with phallacidin (Fig. 8A–B). The entire ground plan of the adult nervous system was established by the 4th day of development. At this stage we were able to distinguish the brain ring—that is, rudiments of the cerebral ganglia—connected by the dorsal and ventral cerebral commis-

sures, encircling the rudiment of the proboscis, and the two lateral nerve cords—one on each side of the midgut (Figs. 4A–D; 5A–B). Subsequent development results in gradual enlargement of all of the mentioned components of the nervous system (Figs. 5C–F; 6A–F; 7A, C–F). The cerebral ganglia and the lateral nerve cords are very large and well visible through the body wall of the 10-day-old juvenile worms (Fig. 1G).

*Musculature.* Sometime between 2 and 4 days of development, body-wall muscles appear just inside of the basal lamina of the epidermis (Fig. 4B). By 5 days, numerous well-differentiated longitudinal and transverse fibers form a complete muscular sheath (Fig. 5). A thin layer of diagonal muscles develops between the outer circular and the inner longitudinal body-wall muscle layers by 8 days after fertilization (Fig. 7B).

Additionally, we could distinguish two strands of longitudinal muscle fibers running along the inner side of the lateral nerve cords and passing through the brain ring in 5- and 8-day-old larvae (Figs. 6B–C, E; 7A, C, E) and in 10-day- and 2-week-old juveniles (data not shown). Such nerve cord muscles are very common in hoplonemerteans and can be observed on histological sections of the adults in many monostiliferan and polystiliferan species (*e.g.*, Coe, 1943, p. 152; Maslakova *et al.*, 2005; Maslakova and Norenburg, 2008a, b). Proboscis insertion muscles develop by 8 days after fertilization (Fig. 7C–D).

### *Transitory epidermis in embryonic and larval development of the hoplonemerteans* Antarctonemertes phyllospadicola *and* Oerstedia dorsalis

The characteristic V-shaped parchment-like egg cocoons of *A. phyllospadicola* that we collected were up to 10 mm long (Fig. 9A) and typically found attached to retinacules (leaf-like structures covering ovaries) inside the mature female inflorescences of surfgrass *Phyllospadix scouleri*. Each cocoon contained 5–27 (average 13.8, $n = 35$) yolky yellowish to orange eggs round to oval in shape (310–375 $\mu$m in diameter) and enclosed in tight extracellular egg chorions, or embryos at various stages of development. Eggs and embryos were embedded in a viscous gelatinous matrix filling the cocoon. We found at least three other species of small, pale, nondescript four-eyed hoplonemerteans co-occurring with *A. phyllospadicola*, but all the cocoons we collected were of the same kind. We confirmed that the cocoons we collected in the field were those of *A. phyllospadicola*, by comparing them to the cocoons laid in captivity by the reproductive adults of *A. phyllospadicola* collected from the surfgrass flowers at the same location. Frequently, we found one or more adults of *A. phyllospadicola* and up to three egg cocoons inside a single inflorescence.

Development of this species is entirely encapsulated and takes several weeks from cocoon deposition to the emergence of juveniles from the cocoons (we have not determined the exact duration of embryonic development). About a week or two after cocoon deposition, the embryos hatch from the extra-embryonic chorions, but they remain inside the cocoon for several more weeks. The surface of such hatchlings appears lumpy in reflected light under the dissecting microscope or dark-field compound microscope due to the large cells of the transitory epidermis, visible through the semitransparent wall of the egg cocoon (Fig. 9B). As in the larvae of *Paranemertes peregrina* described above, the cells of the embryonic epidermis in *A. phyllospadicola* look dramatically different from the cells of the definitive epidermis in confocal Z-projections of phallacidin-labeled hatchlings; the difference is due not only to their larger size but also their brighter phallacidin staining, which suggests that the cortex of these cells is relatively stable, which, in turn, hints at lack of mitotic activity (Fig. 9C). Thus it appears that the cells of the larval epidermis in *A. phyllospadicola* are also cleavage-arrested. We observed with light microscopy that hatchlings dissected out of the cocoons are sparsely and non-uniformly ciliated. It appears that the large cells of the embryonic epidermis lack cilia altogether, while cells of the definitive epidermis have short cilia. This pattern of ciliation was confirmed by the scanning electron microscopy (Fig. 9D–E) and confocal microscopy of hatchlings double-labeled with phallacidin and anti-tubulin antibody (Fig. 9F–G).

A similar structure was observed in the planktonic development of the hoplonemertean *Oerstedia dorsalis*. Large cells of the transitory larval epidermis gave the 2-day-old planuliform planktonic larva the bumpy appearance of a pickling cucumber, reminiscent of that of the *Antarctonemertes phyllospadicola* embryos removed from the egg cocoon. SAM observed a few cells of the larval epidermis in the process of being shed by the 2-day-old larvae that were slightly compressed under a coverslip.

## Discussion

### *Transitory epidermis in larval development of hoplonemerteans*

Development with a transitory epidermis appears to be widespread among the hoplonemerteans but may have escaped notice in many classical studies. Our interpretation of the literature indicates that at least seven hoplonemertean species from a broad taxonomic range possess a transitory epidermis: *Tetrastemma vermiculus* and *Drepanophorus spectabilis* (Lebedinsky, 1898), *Emplectonema gracile* (Delsman, 1915), *Prostoma graecense* (Reinhardt, 1941), *Argonemertes australiensis* (Hickman, 1963), *Tetrastemma candidum* (Maslakova and Malakhov, 1999), and *Prosadenoporus floridensis* (Maslakova and Norenburg, 2008a). Another recent study reported the presence of the transitory

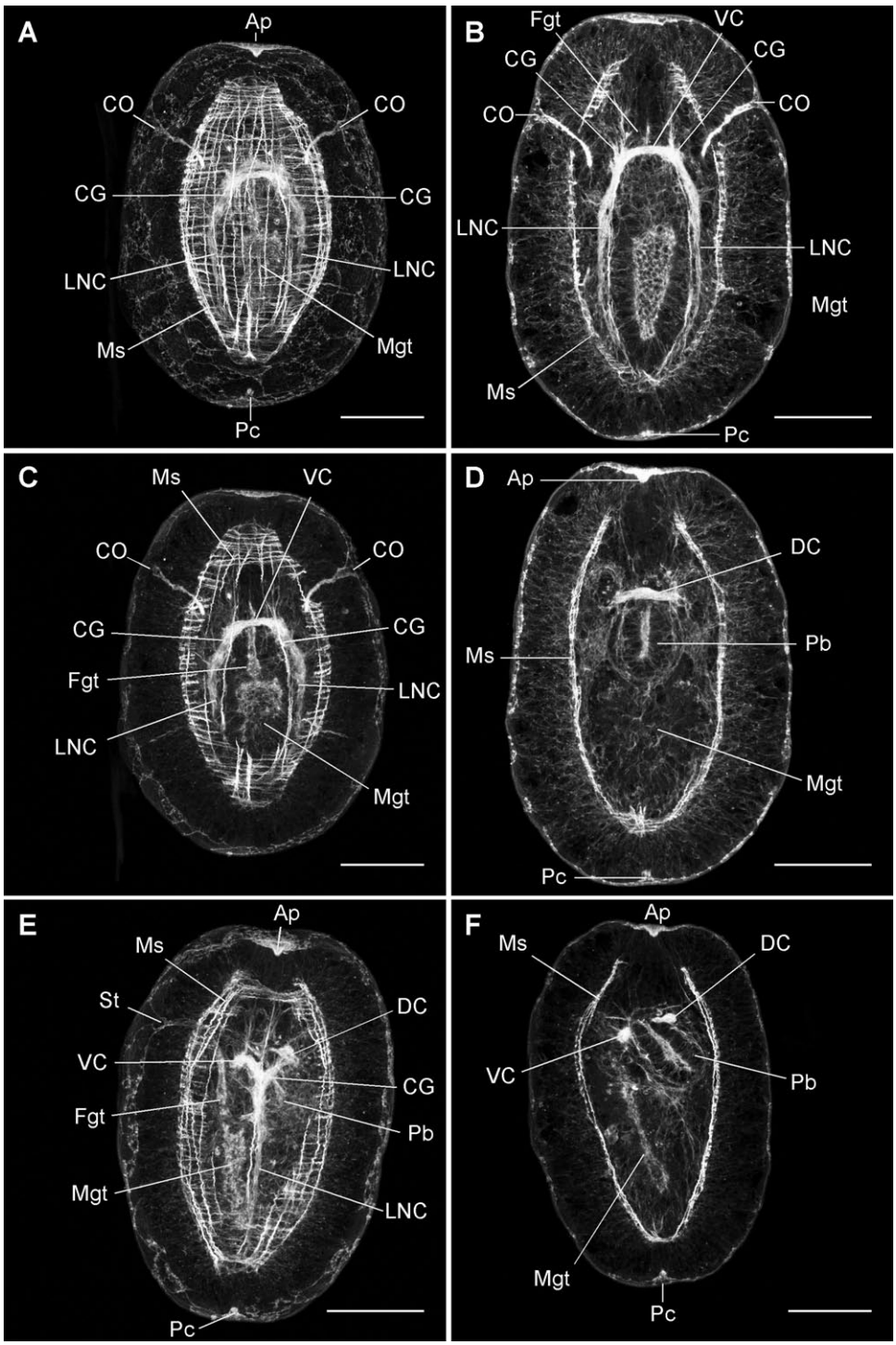


**Figure 6.** Internal anatomy of the phallacidin-labeled 5-day-old larvae of *Paranemertes peregrina* revealed in confocal z-projections of sub-stacks of 1-$\mu$m optical sections, chosen to illustrate major morphological structures. The longitudinal and circular body-wall muscles (Ms) are well developed in the 5-day-old larvae. Anterior end, marked by the apical organ (Ap), is up. (A) Frontal sections, complete stack of sections of the entire larva. (B) Frontal sections, 10 $\mu$m sub-stack. The cerebral organs (CO) penetrate the body wall, and their distal portions lie close to cerebral ganglia (CG). (C) Frontal sections, same specimen as in A, 20-$\mu$m sub-stack. The foregut (Fgt) and the midgut (Mgt) fused to form a continuous lumen. (D) Frontal sections, same specimen as in B but a different 10-$\mu$m sub-stack. A thin layer of tissue around the proboscis (Pb) likely represents the

epidermis in the larval development of *Quasitetrastemma stimpsoni* (Magarlamov and Chernyshev, 2009). We report transitory epidermis in *Paranemertes peregrina*, *Antarctonemertes phyllospadicola*, and *Oerstedia dorsalis*. Additionally, SAM recently observed a similar structure in planuliform larvae of *Pantinonemertes californiensis*, bringing the total up to 12 species. It is likely that this developmental type represents the rule rather than an exception for hoplonemerteans.

The transitory epidermis of the planuliform larva of *Paranemertes peregrina* is composed of about 90 large multiciliated cleavage-arrested cells, which are gradually replaced by the much more numerous and smaller intercalating cells of the definitive epidermis. Cells of the larval epidermis appear to cytolyse, rather than being simply shed as appears to be the case in larvae of *Oerstedia dorsalis* and *Pantinonemertes californiensis* (Maslakova, pers. obs.). Definitive epidermis includes a variety of cell types, such as multiciliated cells and various gland cells. The transition from swimming to crawling happens within the first 10 days of development in *P. peregrina* and coincides with the replacement of larval epidermis by the definitive epidermis.

In general, multiciliated cells cannot divide because, if the many basal bodies were to behave as centrosomes, assembly of a bipolar spindle would be challenging. Therefore, for the epidermis to undergo a continuous renewal there must be some cells that are not multiciliated. What is remarkable about the cells of larval epidermis is not that they are cleavage-arrested, for most multiciliated cells presumably would be. What is remarkable is that these cells are relatively large; have distinctly different nuclei; and cover almost the entire surface in newly hatched larvae, then disappear as a single generation. The fact that the cells of the larval epidermis are very large suggests that they become cleavage-arrested early in development, develop numerous cilia, and are dedicated to swimming. Allocating a few cells early in development to locomotion allows the progenitors of the definitive epidermis to continue cell division and differentiate into the diverse cell types of the "crawling" epidermis, while the larva is swimming.

It is interesting that development with a transitory epidermis is also found in hoplonemerteans that have encapsulated development and lack a swimming stage, such as *Tetrastemma candidum* (Maslakova and Malakhov, 1999), *Argonemertes australiensis* (Hickman, 1963), *Prosadenoporus floridensis* (Maslakova and Norenburg, 2008a), and *Antarctonemertes phyllospadicola* (present study). In the latter, the cells of the transitory epidermis lack cilia altogether. This could be interpreted as a nonfunctional remnant of the larval epidermis (implying that the ancestor had a swimming larva), or possibly as a remnant that acquired a new function, for example, yolk storage. Alternatively, the widespread conservation of the transitory epidermis among nonswimming hoplonemerteans may suggest some more significant function or developmental role, the elucidation of which will require a detailed comparative study of early morphogenesis and cell lineage.

In many spiralians, the function of early swimming is taken by the differentially ciliated cells of the prototroch, ranging in number from 28 to 40 cells (Damen and Dictus, 1994). In the palaeonemertean *Carinoma*, the hidden prototroch consists of 40 multiciliated cells that cover nearly the entire larval surface at the time of hatching. They gradually reduce their coverage by forming a compact equatorial band, while the multiciliated cells of the definitive epidermis progressively take up more and more surface area (Maslakova *et al*., 2004a, b). Similar events, which involve the shedding or histolysis of the larval epidermis variously called "serosa" or "test," occur during development of some other spiralians, for example the stenocalymma larva of the scaphopod mollusc *Dentalium* (Lacaze-Duthiers, 1856; after Buckland-Nicks *et al.*, 2002), the test larva of neomenioid aplacophorans (Thompson, 1960; Okusu, 2002), and the pericalymma of the protobranch bivalve molluscs (Gustafson and Reid, 1986; Gustafson and Lutz, 1992; Zardus and Morse, 1998), as well as the unusual larva of the sipunculid *Sipunculus nudus* (Gerould, 1903; Rice, 1988). In each of these, the cells presumed to be derived from the trochoblast lineage originally cover nearly the entire larval surface and disappear as a distinct preoral domain during the course of larval development.

In contrast, the cells of the hoplonemertean transitory epidermis become separated from each other by the intercalating cells of the definitive epidermis, like continents drifting apart in a sea of small cells. While the hoplonemertean transitory epidermis might be derived in part from the trochoblast cell lineage, it is likely that other lineages contribute as well, judging from the large number of participating cells. Especially in light of *Carinoma*'s prototroch, it will be of considerable interest to determine the hoplonemertean cell lineage by using intracellular markers. This will also reveal whether the progenitors of the definitive epidermis originate from intermediate lineages, ingress between the cells of the larval epidermis, proliferate, and later are admitted to epidermis again; or whether they originate from an entirely different lineage, ingress during gastrulation, and later intercalate between the resorbing cells of the larval epidermis.

The original motivation to study palaeonemertean and hoplonemertean transitory epidermis was a hypothesis that it may represent a remnant of the pilidial development in the

rudiment of the rhynchocoel. (E) Sagittal sections, 30-$\mu$m sub-stack. (F) Sagittal sections, different specimen from E, 10-$\mu$m sub-stack. Scale bars 50 $\mu$m. DC, dorsal brain commissure; LNC, lateral nerve cord; Pc, posterior cirrus; St, mouth; VC, ventral brain commissure.

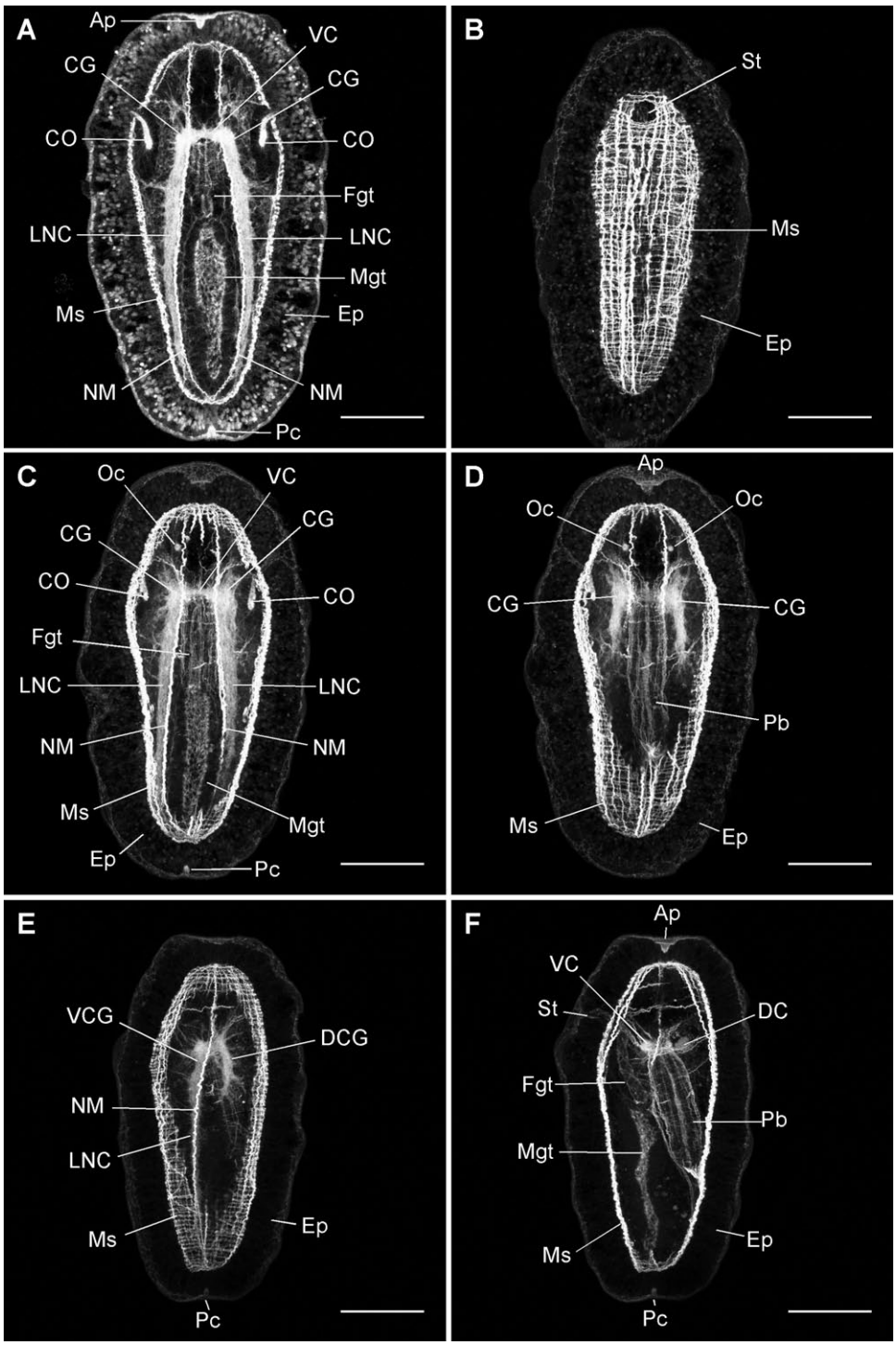


**Figure 7.** Internal anatomy of the phallacidin-labeled (unless otherwise noted) 8-day-old larvae of *Paranemertes peregrina* revealed in confocal z-projections of sub-stacks of 1-$\mu$m optical sections. Compared to the 4- and 5-day-old larvae, these are more elongated and have more body-wall musculature (Ms): in addition to circular and longitudinal muscles, one can discern a few diagonal muscle fibers. In addition, there are the proboscis (Pb) muscles, and two thick strands of muscles (NM) that run along the inner side of the lateral nerve cords (LNC). Apical pole (Ap) is up. (A) Frontal sections, 5-$\mu$m sub-stack of a larva double-labeled with phallacidin and Sytox Green (nuclear stain). The foregut (Fgt) and the midgut (Mgt) are fully integrated and have a continuous lumen. The cerebral ganglia (CG) and lateral nerve cords (LNC) have massive fibrous cores and occupy a large amount of space inside the body wall. (B) Frontal sections, 10-$\mu$m sub-stack. (C–D) Frontal

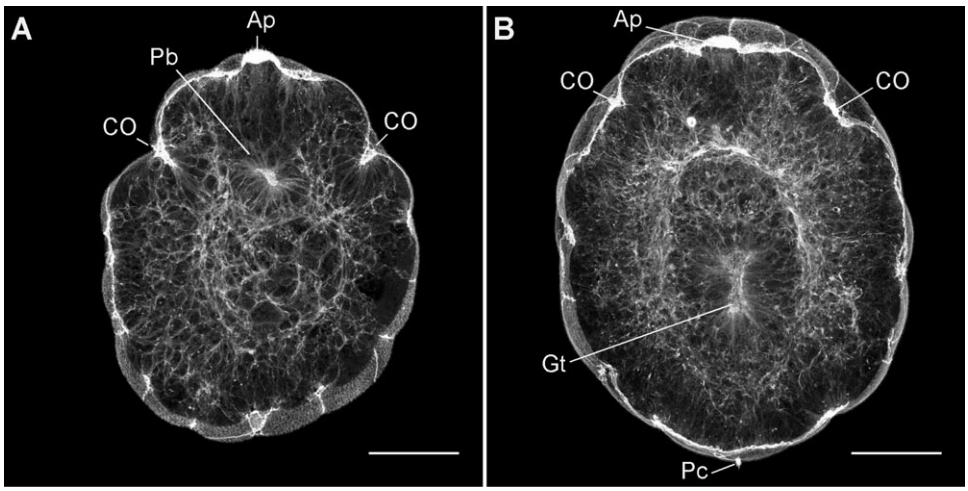


**Figure 8.** Internal anatomy of the phallacidin-labeled 2-day-old larvae of *Paranemertes peregrina* revealed in confocal z-projections of sub-stacks of 1-$\mu$m optical sections. The anterior end (up) is marked by the apical organ (Ap); the posterior end, by the posterior cirrus (Pc). Frontal sections. (A) A 10-$\mu$m sub-stack. The proboscis (Pb) appears as an internal spherical mass of tissue with a small lumen, which does not have an obvious connection to the outside. The two anterolateral invaginations are the nascent cerebral organs (CO). (B) A 45-$\mu$m sub-stack from a different specimen. The gut (Gt) appears to have no connection to the outside at this stage. Scale bars 50 $\mu$m.

ancestral nemertean. This turned out not to be the case in the palaeonemertean species *Carinoma tremaphorus* (Maslakova *et al*., 2004a, b); instead we discovered a vestigial prototroch. The hoplonemertean transitory epidermis looks and behaves differently from the modified prototroch in *Carinoma*. We cannot entirely dismiss the possibility that the hoplonemertean larval epidermis is a remnant of the pilidial body; however, it is also possible that it served as a precursor of the pilidial development. Determination of the cell lineage by using intracellular markers and comparison with the pilidiophoran species that have lost the pilidium secondarily—for example *Poseidon viridis, Poseidon ruber,* and *Micrura akkeshiensis*—will likely help to clarify the direction of evolutionary transition between the hoplonemertean and pilidiophoran larval epidermis.

### *Organogenesis in hoplonemerteans*

In adult hoplonemerteans the gut is divided into two histologically and functionally distinct regions, the midgut and the foregut. The foregut and the proboscis pore open into the rhynchodeum, which connects to the outside *via* a rhynchostomopore (a combined opening of mouth and proboscis). Foregut development is described differently in nearly every study of hoplonemertean development to date. Some suggest that it appears as a separate invagination, then closes again and opens into the invaginating rhynchodeum, while others describe it as an outpocketing of the ectodermal rhynchodeum (reviewed in Friedrich, 1979). We found that in *Paranemertes peregrina*, the blastopore closes completely and the foregut develops as a separate invagination on the ventral side of the planuliform larva, independent of the proboscis or rhynchodeum. The foregut extends back and connects to the midgut.

Contrary to the previous reports on hoplonemertean development (Friedrich, 1979), we did not observe an actual invagination associated with the developing proboscis in *Paranemertes*. Instead it first became apparent at the anterior end of the larva as an internal mass of cells in which a lumen emerged progressively and later joined the foregut to form a common rhynchodeum. However, it is possible that we missed the invagination of proboscis rudiment if it happens before hatching, lacks an obvious lumen initially, and closes by 50 h of development.

Two other prominent epidermal invaginations form laterally at the anterior end. These are the rudiments of the

sections, same individual, different 20-$\mu$m sub-stacks. Two ocelli (Oc) are visible anterior to the brain in D. (E–F) Sagittal sections, same individual, different 15-$\mu$m sub-stacks. The proboscis reached about one-third of the body length. Scale bars 50 $\mu$m. CO, cerebral organ; DC, dorsal brain commissure; DCG, dorsal cerebral ganglion; St, mouth; Pc, posterior cirrus; VC, ventral commissure of cerebral ganglia; VCG, ventral cerebral ganglion.

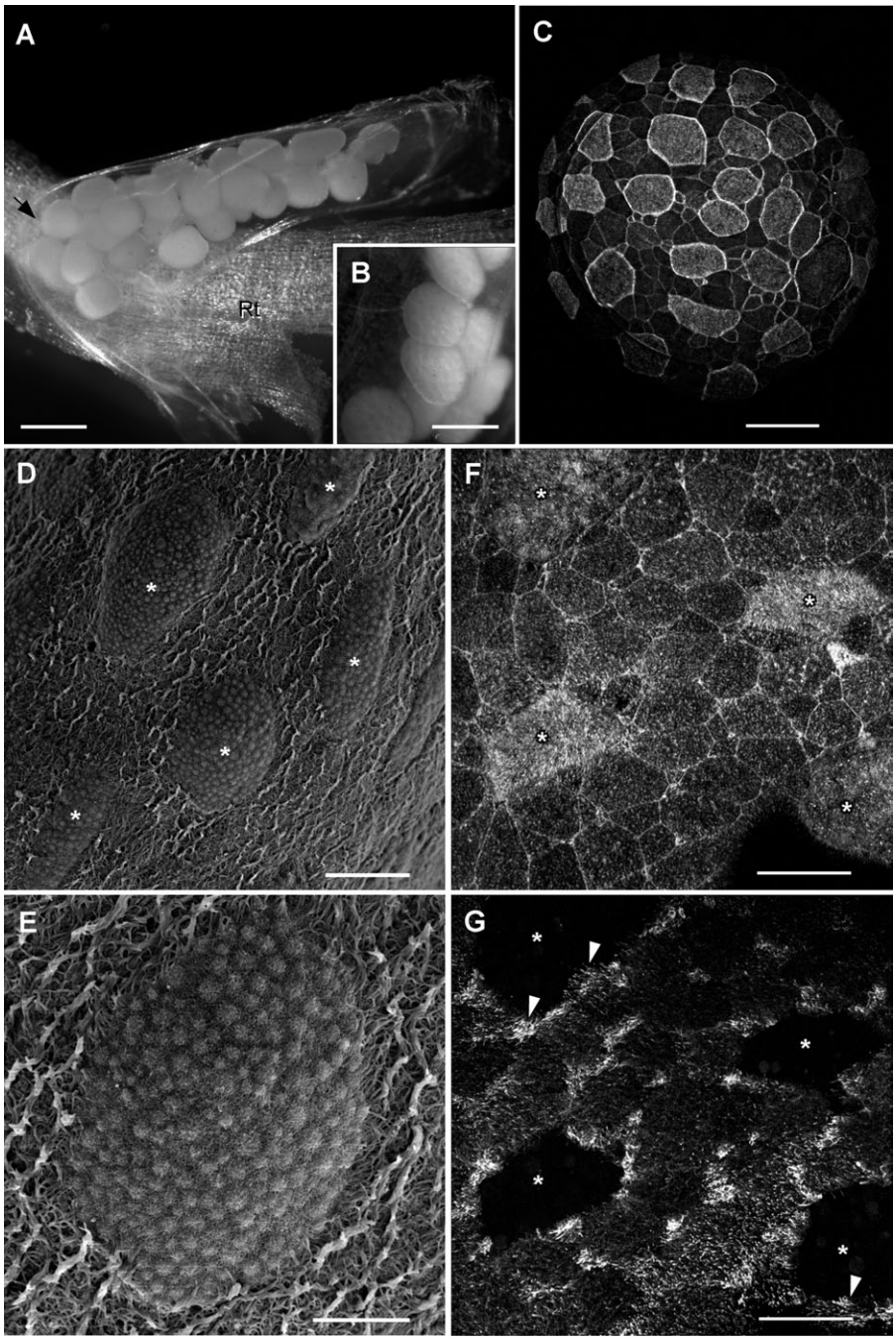


**Figure 9.** Cocoons and embryos of *Antarctonemertes phyllospadicola* in various stages of resorbing the cells of the embryonic epidermis. (A) Characteristic V-shaped cocoon attached to a flower retinacule (Rt) of surfgrass *Phyllospadix scouleri*. Apex of the "V" marked with an arrow. Scale bar 0.5 mm. (B) Embryos, at least 1- or 2-weeks-old, hatched from the egg chorions, photographed through the wall of the cocoon; the lumpy appearance of the embryos is due to the presence of the large cells of embryonic epidermis. Scale bar 350 $\mu$m. (C) Confocal projection of a phallacidin-labeled embryo (about the same stage as in B) showing the brightly labeled large cells of embryonic epidermis separated by the smaller and less intensely stained cells of the definitive epidermis. Some cells of the embryonic epidermis reach up to 50–75 $\mu$m across and still share borders. Scale bar 75 $\mu$m. (D) Scanning electron microscopy (SEM) image of a more advanced embryo than in C, showing large nonciliated cells of the embryonic epidermis (asterisks), densely covered with microvilli and bumpy with what we interpret as protruding yolk granules, completely surrounded by the sparsely ciliated (cilia are short and matted down) expanse of the definitive epidermis. Scale bar 25 $\mu$m. (E) SEM image of one of the cells of the

cerebral organs, which remain open to the outside throughout larval and juvenile development and into adulthood. The cerebral organs are among the first recognizable structures in the larva of *Paranemertes peregrina,* and as such, represent important anatomical landmarks. Another prominent anterior structure, which sometimes appears slightly invaginated, is the apical organ. We suspect that the apical and cerebral organs were often mistaken for proboscis or rhynchodeal invaginations (*e.g.,* Hammarsten, 1918; Iwata, 1960), nervous system rudiments (Maslakova and Malakhov, 1999), or frontal organ or cephalic gland anlagen (Lebedinsky, 1898) in earlier studies. According to our observations, the nervous system in *P. peregrina* is not associated with any epidermal invaginations.

Interestingly, two anterolateral invaginations, interpreted as nervous system rudiments, are described in the development of several palaeonemertean species: *Cephalothrix rufifrons* (Smith, 1935); *Procephalothrix filiformis*, *Procephalothrix simulus,* and *Tubulanus punctatus* (Iwata, 1960); and *Carinoma tremaphoros* (Maslakova *et al*., 2004b). Their position and developmental timing resemble those of cerebral organ rudiments in *Paranemertes*, not nervous system rudiments. As adults, all of these palaeonemerteans, except *Tubulanus*, lack cerebral organs. Correspondingly, the presumed cerebral organ rudiments exist for only a short time and disappear without a trace (Iwata, 1960; Maslakova *et al*., 2004b). Likewise, Hammarsten (1918) identified two transitory anterolateral epidermal invaginations as rudiments of cerebral organs in the development of *Malacobdella grossa,* a highly modified hoplonemertean that is a commensal in the mantle cavity of bivalve molluscs, which lacks cerebral organs as an adult. If these anterior invaginations indeed are vestiges of cerebral organs, it would support the hypothesis of the secondary loss of cerebral organs in *Malacobdella* and many palaeonemerteans and the homology of the cerebral organs across the phylum.

Development with a swimming larva was known for *Paranemertes peregrina* (Roe, 1976), but larval morphology, anatomy, and the presence of the transitory epidermis are described here for the first time. This is also the first time that hoplonemertean development has been described using fluorescent labeling and confocal microscopy; all previous studies were based on traditional histological sections. Fluorescent phalloidin, in combination with confocal laser scanning microscopy, is singularly useful for studying epidermal dynamics. This method allowed us to document the otherwise inconspicuous process of epidermal replacement in the uniformly ciliated planktonic larvae of *P. peregrina*, as well as the development of all major hoplonemertean organ systems, with a more robust dataset than previously used in conventional histological analyses.

### *Note on taxonomy of* Antarctonemertes phyllospadicola *(Stricker, 1985)*

Originally described as *Tetrastemma phyllospadicola* by Stricker (1985), this species was transferred to *Antarctonemertes* Friedrich by a Russian nemertinologist, Chernyshev, who pointed out that this species has short accessory nerves in the lateral nerve cords (Stricker, 1985: p. 686., fig. 12) and lacks a rhynchocoelic vascular plug (Chernyshev, 1999). Apparently, well-developed mucous cephalic glands penetrating an otherwise "closed" precerebral septum also unite this species with *Antarctonemertes* (Chernyshev, 1999). Because well-developed cephalic glands and presence of the accessory nerves are certainly not unique to the hoplonemertean genus *Antarctonemertes* and because the phylogeny of neither *Tetrastemma*, *Antarctonemertes* nor related genera has been reconstructed using morphological or molecular cladistic analysis, it is uncertain at which level the above-mentioned characters constitute synapomorphies and whether they are appropriate for assigning hoplonemertean species to any particular genus. Regardless of whether this taxonomic placement is defensible on philosophical grounds or not, it is supported by our cytochrome oxidase I sequence data, which suggest a close relationship between *A. phyllospadicola* and another small, nondescript, four-eyed hoplonemertean from the Sea of Japan—*Antarctonemertes varvarae* Chernyshev 1999 (the closest match of all nemertean COI sequences available in GenBank). The uncorrected sequence divergence was 10%, which is comparable to the divergence between the COI sequences of morphologically distinguishable congeneric species in well-defined by the morphological and molecular characters, monophyletic genera of hoplonemerteans such as *Prosadenoporus* and *Prosorhochmus* (Maslakova and Norenburg, 2008a, b).

## Acknowledgments

Most of the work was carried out at the University of Washington's Friday Harbor Laboratories (Friday Harbor, WA), and we thank the FHL faculty and staff for their generous support throughout the years. We are grateful to the members of the Center for Cell Dynamics for access to

embryonic epidermis from above, enlarged. Scale bar 10 $\mu$m. (F and G) Confocal image of the surface of an embryo further along in development than in D and E, double-labeled with phallacidin (F) and anti-tubulin antibody (G). Note the four degenerative cells of the embryonic epidermis (asterisks) brightly labeled with phallacidin (F) but left unstained by the anti-tubulin antibody (G), in contrast to the surrounding cells of the definitive epidermis which bear numerous very short cilia (arrowheads). Scale bars 30 $\mu$m.

the confocal microscope, and in particular, to Dr. George von Dassow for help with the equipment, image processing, and comments on the manuscript. TEM was done by JvD at Freie Universität Berlin, Germany. SEM was done at the Oregon Institute of Marine Biology (Charleston, OR). We thank the director of the OIMB, Dr. Craig Young, for providing access to the SEM equipment, and Dr. Tracey Smart for training and help with it. SAM is grateful to Dr. Mark Martindale for the opportunity to work at the Marine Biological Laboratory in Woods Hole in 2000 and to Dr. Jon Norenburg and Dr. Mary Rice (Smithsonian Institution) for supporting her embryological pursuits while a Ph.D. student in systematics. SAM was assisted by the students of the OIMB Marine Molecular Biology class 2008 (Laurel Hiebert, Kenta Tsutsui, and Sara Wykoff) in obtaining the sequence data from *Antarctonemertes phyllospadicola*. SAM was supported by the Friday Harbor Labs postdoctoral fellowship. JvD was supported by the German Research Council (Grant # BA 1520/11-1).

## Literature Cited

**Buckland-Nicks, J., G. Gibson, and R. Koss. 2002.** Phyllum Mollusca: Polyplacophora, Aplacophora, Scaphopoda. Pp. 245–260 in *Atlas of Marine Invertebrate Larvae*, C. M. Young, M. A. Sewall, and M. E. Rice, eds. Academic Press, San Diego.

**Cantell, C.-E. 1966.** The devouring of the larval tissues during the metamorphosis of pilidium larvae (Nemertini). *Ark. Zool.* **18:** 489–492.

**Cantell, C.-E. 1969.** Morphology, development and biology of the pilidium larvae (Nemertini) from the Swedish west coast. *Zool. Bidr. Upps.* **38:** 61–111.

**Chernyshev, A. V. 1999.** Nemerteans of the genus *Antarctonemertes* (Enopla, Monostilifera). *Zool. Zh.* **78:** 939–948.

**Coe, W. R. 1899.** Development of the pilidium of certain nemerteans. *Trans. Conn. Acad. Arts Sci.* **10:** 235–262.

**Coe, W. R. 1904.** The anatomy and development of the terrestrial nemertean *Geonemertes agricola* of Bermuda. *Proc. Boston Soc. Nat. Hist.* **31:** 531–570.

**Coe, W. R. 1943.** Biology of the nemerteans of the Atlantic coast of North America. *Trans. Conn. Acad. Arts Sci.* **35:** 129–328.

**Damen, P., and W. J. A. G. Dictus. 1994.** Cell lineage of the prototroch of *Patella vulgata* (Gastropoda, Mollusca). *Dev. Biol.* **162:** 364–383.

**Dawydoff, C. 1940.** Les formes larvaires de Polyclades et de Némertes du plancton Indochinois. *Bull. Biol. Fr. Belg.* **74:** 443–496.

**Delsman, H. 1915.** Eifurchung und Gastrulation bei *Emplectonema gracile* Stimpson. *Tijdschr. Ned. Dierk. Vereen.* **14:** 68–114.

**Folmer, O., M. Black, W. Hoeh, R. Lutz, and R. Vrijenhoek. 1994.** DNA primers for amplification of mitochondrial cytochrome c oxidase subunit I from diverse metazoan invertebrates. *Mol. Mar. Biol. Biotechnol.* **3:** 294–299.

**Friedrich, H. 1979.** *Morphogenese der Tiere. Nemertini*. Gustav Fischer, Jena.

**Gerould, J. H. 1903.** *Studies on the Embryology of the Sipunculidae. I. The Embryonal Envelope and its Homologue*. Henry Holt, New York.

**Gustafson, R. G., and R. A. Lutz. 1992.** Larval and early postlarval development of the protobranch bivalve *Solemya velum* (Mollusca, Bivalvia). *J. Mar. Biol. Assoc.* **72:** 383–402.

**Gustafson, R. G., and R. G. B. Reid. 1986.** Development of the pericalymma larva of *Solemya reidi* (Bivalvia, Cryptodonta, Solemyidae) as revealed by light and electron microscopy. *Mar. Biol.* **93:** 411–427.

**Hammarsten, O. D. 1918.** Beitrag zur Embryonalentwicklung der *Malacobdella grossa* (Müll.), Inaugural dissertation, Zootomischen Institut der Hochschule zu Stockholm, Almqvist & Wiksells Boktryckeri A. B., Uppsala.

**Hickman, V. V. 1963.** The occurence in Tasmania of the land nemertine, *Geonemertes australiensis* Dendy, with some account of its distribution, habits, variations and development. *Pap. Proc. R. Soc. Tasman.* **97:** 63–75.

**Iwata, F. 1957.** On the early development of the nemertine *Lineus torquatus* Coe. *J. Fac. Sci. Hokkaido Univ. Ser. 6 Zool.* **13:** 54–58.

**Iwata, F. 1958.** On the development of the nemertean *Micrura akkeshiensis. Embryologia* **4:** 103–131.

**Iwata, F. 1960.** Studies on the comparative embrylogy of nemerteans with special reference to their interrelationship. *Publ. Akkeshi Mar. Biol. Stat.* **10:** 1–51.

**Jägersten, G. 1972.** *Evolution of the Metazoan Life Cycle*. Academic Press, New York.

**Lacalli, T. C. 2005.** Diversity of form and behaviour among nemertean pilidium larvae. *Acta Zool.* **88:** 267–276.

**Lacaze-Duthiers, H. 1856.** Histoire de l'organisation et du developpement du Dentale. *Ann. Sci. Nat. (Zoologie), Ser. 4* **VI:** 5–51.

**Lebedinsky, Y. N. 1898.** Nabljudenija nad istoriej razvitija nemertin. *Zapiski Novorossijskogo Obshchestva Estestvoispytatelej* **22:** 1–123.

**Magarlamov, T. Yu., and A. V. Chernyshev. 2009.** Ultrastructure of larval epidermis of the nemertean *Quasitetrastemma stimpsoni* (Chernyshev, 1992) (Hoplonemertea). *Russ. J. Mar. Biol.* **35:** 34–40.

**Maslakova, S. A., and V. V. Malakhov. 1999.** A hidden larva in nemerteans of the order Hoplonemertini. *Dokl. Biol. Sci.* **366:** 314–317.

**Maslakova, S. A., and J. L. Norenburg. 2008a.** Revision of the smiling worms, genera *Prosadenoporus* Bürger, 1890 and *Pantinonemertes* Moore and Gibson, 1981 and description of a new species *Prosadenoporus floridensis* sp. nov. (Prosorhochmidae; Hoplonemertea, Nemertea) from Florida and Belize. *J. Nat. Hist.* **42:** 1689–1727.

**Maslakova, S. A., and J. L. Norenburg. 2008b.** Revision of the smiling worms, genus *Prosorhochmus* Keferstein 1862, and description of a new species, *Prosorhochmus belizeanus* sp. nov. (Prosorhochmidae, Hoplonemertea, Nemertea) from Florida and Belize. *J. Nat. Hist.* **42:** 1219–1260.

**Maslakova, S. A., M. Q. Martindale, and J. L. Norenburg. 2004a.** Fundamental properties of the spiralian developmental program are displayed by the basal nemertean *Carinoma tremaphoros* (Palaeonemertea, Nemertea). *Dev. Biol.* **267:** 342–360.

**Maslakova, S. A., M. Q. Martindale, and J. L. Norenburg. 2004b.** Vestigial prototroch in a basal nemertean, *Carinoma tremaphoros* (Nemertea; Palaeonemertea). *Evol. Dev.* **6:** 219–226.

**Maslakova, S. A., M. Thiel, N. Vasquez, and J. L. Norenburg. 2005.** The smile of *Amphiporus nelsoni* Sanchez, 1973 (Nemertea : Hoplonemertea : Monostilifera : Amphiporidae) leads to a redescription and a change in family. *Proc. Biol. Soc. Wash.* **118:** 483–498.

**McIntosh, W. C. 1873–1874.** *A Monograph of the British Annelids. Part I. The Nemerteans.* Ray Society, London.

**Norenburg, J. L. 1986.** Redescription of a brooding nemertine, *Cyanophthalma obscura* (Schultze) gen. et comb. n., with observations on its biology and discussion of the species of *Prostomatella* and related taxa. *Zool. Scr.* **15:** 275–293.

**Norenburg, J. L., and S. A. Stricker. 2002.** Nemertea. Pp. 163–177 in *Atlas of Marine Invertebrate Larvae*, C. M. Young, M. A. Sewall, and M. E. Rice, eds. Academic Press, San Diego.

**Okusu, A. 2002.** Embryogenesis and development of *Epimenia babai* (Mollusca Neomeniomorpha) *Biol. Bull.* **203:** 87–103.

**Reinhardt, H. 1941.** Beiträge zur Entwiklungsgeschichte der einheimischen Süsswassernemertine *Prostoma graecense* (Böhmig). *Vierteljahrsschr. Naturforsch. Ges. Zuer.* **86:** 184–255.

**Rice, M. E. 1988.** Observations on development and metamorphosis of *Siphonosoma cumanense* with comparative remarks on *Sipunculus nudus* (Sipuncula, Sipunculidae). *Bull. Mar. Sci.* **42:** 1–15.

**Roe, P. 1976.** Life history and predator-prey interactions of the nemertean *Paranemertes peregrina* Coe. *Biol. Bull.* **150:** 80–106.

**Roe, P. 1979.** Aspects of development and occurrence of *Carcinonemertes epialti* (Nemertea) from shore crabs in Monterey Bay, California. *Biol. Bull.* **156:** 130–140.

**Roe, P. 1993.** Aspects of the biology of *Pantinonemertes californiensis*, a high intertidal nemertean. *Hydrobiologia* **266:** 29–44.

**Roe, P., J. L. Norenburg, and S. A. Maslakova. 2007.** Nemertea. Pp. 182–196 in *The Light and Smith Manual: Intertidal Invertebrates from Central California to Oregon*, J. Carlton, ed. University of California Press, Berkeley, CA.

**Salensky, W. 1886.** Bau und Metamorphose des Pilidium. *Z. Wiss. Zool.* **43:** 481–511.

**Salensky, W. 1912.** Morphogenetische Studien an Würmern. II. Über die Morphogenese der Nemertinen. Entwiklungsgeschichte der Nemertine im Inneren des Pilidiums. *Zapiski Imp. Akad. Nauk. St.-Petersburg* **30:** 1–74.

**Salensky, W. 1914.** Morphogenetische Studien an Würmern. II. Die Morphogenese der Nemertinen. 2. Über die Entwicklungsgeschichte des *Prosorochmus viviparus*. *Zapiski Imp. Akad. Nauk. St.-Petersburg* **33:** 1–39.

**Schmidt, G. A. 1964.** Embryonic development of littoral nemertines *Lineus desori* (mihi, species nova) and *Lineus ruber* (O. F. Mülleri, 1774, G. A. Schmidt, 1945) in connection with ecological relation changes of mature individuals when forming the new species *Lineus ruber*. *Zool. Pol.* **14:** 75–122.

**Schwartz, M. L., and J. L. Norenburg. 2005.** Three new species of *Micrura* (Nemertea: Heteronemertea) and a new type of heteronemertean larva from the Caribbean Sea. *Caribb. J. Sci.* **41:** 528–543.

**Smith, J. E. 1935.** Early development of *Cephalothrix*. *Q. J. Microsc. Sci.* **77:** 335–378.

**Stricker, S. A. 1985.** A new species of *Tetrastemma* (Nemertea, Monostilifera) from San Juan Island, Washington, U.S.A. *Can. J. Zool.* **63:** 682–690.

**Stricker, S. A., and C. G. Reed. 1981.** Larval morphology of the nemertean *Carcinonemertes epialti* (Nemertea: Hoplonemertea). *J. Morphol.* **169:** 61–70.

**Thollesson, M., and J. L. Norenburg. 2003.** Ribbon worm relationships: a phylogeny of the phylum Nemertea. *Proc. R. Soc. Lond. B Biol. Sci.* **270:** 407–415.

**Thompson, T. E. 1960.** The development of *Neomenia carinata* Tullberg. *Proc. R. Soc. Lond. B Biol. Sci.* **153:** 263–278.

**von Döhren, J. D., and T. Bartolomaeus. 2006.** Ultrastructure of sperm and male reproductive system in *Lineus viridis* (Heteronemertea, Nemertea). *Zoomorphology* **125:** 175–185.

**Zardus, J. D., and M. P. Morse. 1998.** Embryogenesis, morphology and ultrastructure of the pericalymma larva of *Acila castrensis* (Bivalvia : Protobranchia : Nuculoida). *Invertebr. Biol.* **117:** 221–244.

## Appendix

### Epidermal roll-out maps used in counting cells in *Paranemertes peregrina* larvae

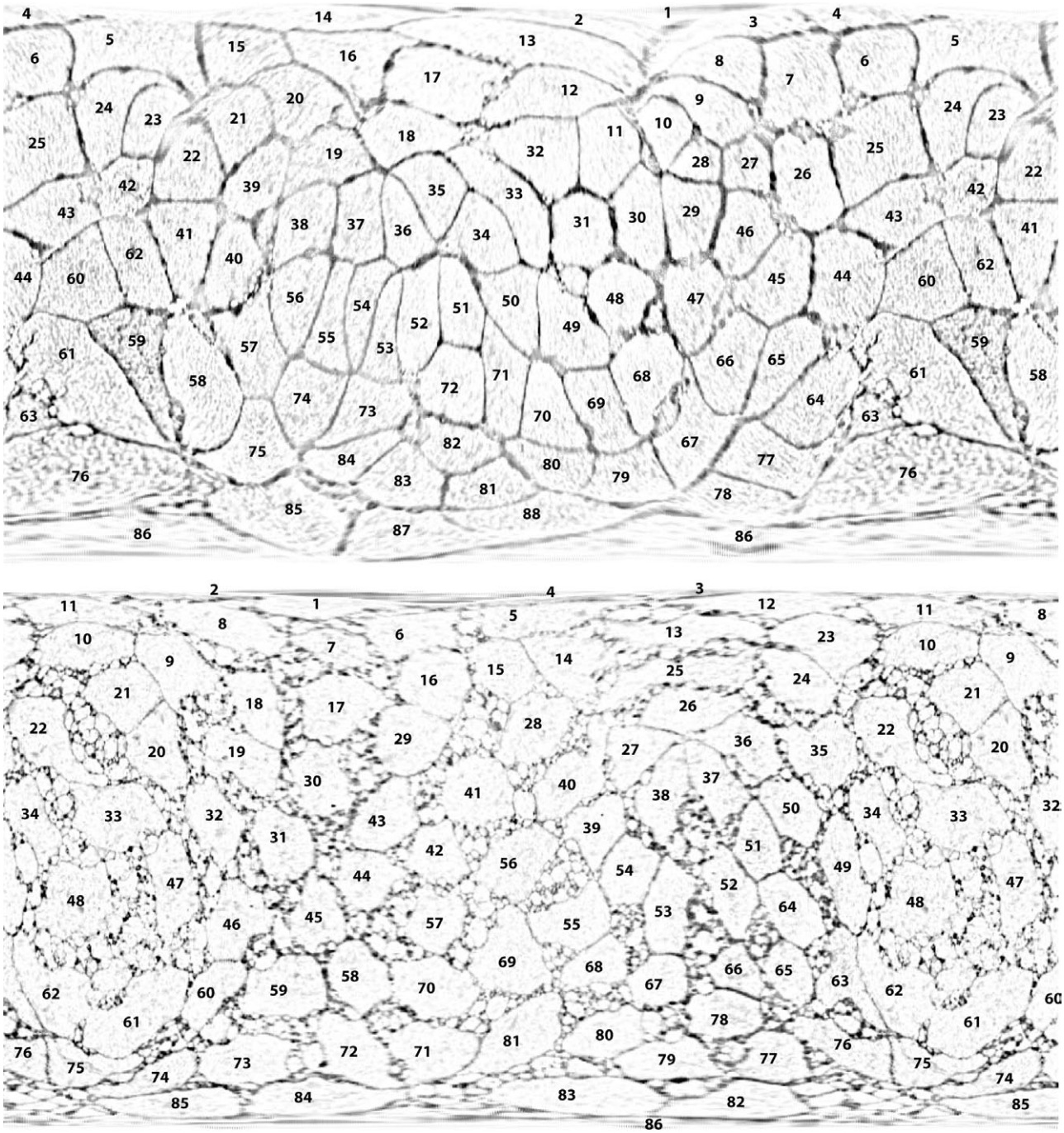

**Appendix Figure 1.** Roll-out maps of epidermis of a 2-day-old (top) and a 5-day-old (bottom) larva of *Paranemertes peregrina;* the maps were created with the help of Voxx and ImageJ software. The numbers are only a counting aid, not an attempt to identify homologous cells in the two larvae. Only the larger cells were counted (88 and 86 in the depicted 2-day-old and 5-day-old larvae, respectively). To generate a flat map of the surface of the embryo, confocal image stacks were first rotated and cropped using ImageJ. A surface rendering was prepared using Voxx, from which a 360-degree rotation at 1-degree increments was exported as a movie. This movie was imported into ImageJ, and a two-pixel-wide strip from the center (the axis of rotation) was excised; to create the map, these 360 two-pixel strips were laid side-by-side, plus 45 degrees worth from each end that were duplicated and added to the left and right to ensure that all cells were represented completely. To facilitate cell counts, background was subtracted in ImageJ using a rolling ball size of 10. Counts were performed by annotating the map while examining the 3-D rendering in Voxx.